A Thermodynamic Investigation of the Melting of B–Z Junction Forming DNA Oligomers†

Richard D. Sheardy,*,‡ Norman Levine,‡ Stephen Marotta,‡ Dongchul Suh,§ and Jonathan B. Chaires§

Department of Chemistry, Seton Hall University, South Orange, New Jersey 07079, and Department of Biochemistry, University of Mississippi Medical School, Jackson, Mississippi 39216-4505

Received July 26, 1993; Revised Manuscript Received December 3, 1993⊗

ABSTRACT: Ultraviolet absorbance methods were used to characterize the thermodynamics of melting of a series of 16 bp deoxyoligonucleotides over a wide range of NaCl concentrations (0–4.5 M) and to obtain complete thermodynamic profiles for their melting at 0.115 and 4.5 M NaCl. The sequence of the series (one strand of duplex) was: 5′-*CGCGCGCG*AMNGACTG-3′, where *C* indicates m^5dC and -MN- was varied to include all combinations of Py:Py stacks (CC, TT, CT, TC). The unmethylated deoxyoligonucleotide 5′-CGCGCGCGACTGACTG-3′ was used as a control sequence. All of the methylated oligonucleotides studied undergo a NaCl-induced transition to a hybrid form containing a left-handed, Z-DNA, region joined to a right-handed region by a B–Z junction. Our experiments allowed us to quantitatively evaluate the effects of NaCl, sequence, and methylation and the transition to the hybrid BZ structure on DNA thermal stability. We found that alteration of a single dinucleotide step has profound effects on the thermal stabilities of the 16 bp fragments studied. Methylation was found to destabilize the double helix, resulting in a decrease in T_m. Transition to the hybrid BZ structure, somewhat surprisingly, was found to only slightly destablize DNA, with an observed decrease in free energy of melting of approximately 0.5 kcal/mol relative to the control, right-handed, sequence in high salt. Transition melting temperatures (T_m) were found, in agreement with previous studies on polymeric DNA, to depend upon NaCl concentration in a complicated, nonlinear fashion. T_m values increase to maximal values at *circa* 1.0 M NaCl, but decrease thereafter with further addition of salt. Our experiments provide quantitative data that help to describe the factors contributing to the stability of the DNA double helix and that document the ability of DNA to accommodate an unusual structure, the B–Z junction, with little energetic cost to its stability.

The conformation of DNA is strongly dependent upon both its sequence and environment. Research in the last decade has shown that DNA can adopt a variety of unusual conformations in response to changes in solution conditions. In addition to global changes in DNA secondary structure (e.g., A, Z-DNA), more localized conformational transitions have been documented (e.g., bends, bulges, junctions). In order to focus on these unusual local DNA conformations, which may occur infrequently in natural genomes, we have designed, synthesized, and characterized model systems based upon short (16–80 bp) pieces of DNA. Our investigations have focused primarily upon the structure and reactivity of DNA oligomers capable of forming B–Z conformational junctions (Sheardy, 1988; Sheardy & Winkle, 1989; Doktycz et al., 1990; Winkle & Sheardy, 1990; Sheardy, 1991; Lu et al., 1992; Sheardy et al., 1993).

One approach to probe the structure of the B–Z junction is to study its interactions with a variety of ligands. The DNA used for such studies has been either BZ–I or BZ–II (Figure 1). Both of these molecules are fully right-handed under conditions of low salt (<0.5 M NaCl), but each undergoes a salt-induced transition to a hybrid conformation possessing both Z and B form segments separated by a B–Z junction (Sheardy, 1988; Sheardy, 1991; Sheardy et al., 1993). The results of ligand binding studies show that B–Z junction forming molecules have unusual ligand reactivity in both low and high salt conditions (Suh et al., 1991; Guo et al., 1991; Ichikawa et al., 1992). Furthermore, the cutting by *Mbo*I of a B–Z junction forming oligomer with an *Mbo*I site at the junction site is enhanced when the junction is present (Winkle et al., 1991). It thus seems apparent that junction formation enhances the binding of certain drugs and restriction endonucleases to DNA oligonucleotides containing the structure, although the detailed mechanisms operative in these cases remain to be defined.

BZ-I:

(C*-G)$_4$--A-C-T-G--(A-C-T-G)
(G-C*)$_4$--T-G-A-C--(T-G-A-C)

BZ-II:

(C*-G)$_4$--A-T-C-G--(A-C-T-G)
(G-C*)$_4$--T-A-G-C--(T-G-A-C)

BZ-V:

(C*-G)$_4$--A-T-T-G--(A-C-T-G)
(G-C*)$_4$--T-A-A-C--(T-G-A-C)

BZ-VI:

(C*-G)$_4$--A-C-C-G--(A-C-T-G)
(G-C*)$_4$--T-G-G-C--(T-G-A-C)

FIGURE 1: The synthetic DNA oligomers of this study where C8 is 5-methylcytidine (m^5dC). The permutations in sequence occur at base pairs 10 and 11. Component strands and corresponding duplexes were prepared as described in Materials and Methods.

† Supported by NSF Grant DMB-8996232 (R.D.S.) and NIH Grant CA35635 (J.B.C.).

* Author to whom correspondence should be addressed.
‡ Seton Hall University.
§ University of Mississippi Medical School.

⊗ Abstract published in *Advance ACS Abstracts,* February 1, 1994.

0006-2960/94/0433-1385$04.50/0 © 1994 American Chemical Society

We have previously reported for BZ–I that the mid-point of the salt-induced transition, determined by monitoring the change in the CD molar ellipticity at 295 nm, can be used to evaluate the free energy of junction formation, ΔG_J (Doktycz et al., 1990). The salt-induced transitions for all oligomers of Figure 1, including the pure Z-forming oligomer $(m^5dC\text{-}dG)_4$, have recently been analyzed (Sheardy et al., 1993). Circular dichroism spectroscopy was used in these studies, along with the method of singular value decomposition, to rigorously establish the number of significant spectral species involved in the B to Z transition. The results showed that the transition is not a simple two-state process, but rather follows a sequential, three-step mechanism, B $\rightleftarrows$ I $\rightleftarrows$ BZ. The intermediate I was proposed to be a partially dehydrated, right-handed conformer. The free energy of junction formation, ΔG_J, was obtained from the data and was found to be dependent on the dinucleotide sequence near the junction location. For the sequences shown in Figure 1, ΔG_J in 4.5 M NaCl was found to vary in the order (from least to most energetically favorable) BZ–V > BZ–II > BZ–I > BZ–VI.

Since enzyme-mediated denaturation of a localized segment of DNA is a prerequisite to DNA replication or transcription, it is of interest to determine the thermodynamic stability of DNA oligomers containing unusual structures. Unusual DNA structures are of interest because they may act as recognition sites for DNA binding proteins. Thermodynamic studies of the stablity of a wide variety of usual and unusual DNA structures have been carried out by a number of investigators (Breslauer et al., 1986; Manzini et al., 1987; Jacobs et al., 1988; Marky et al., 1988; Senoir et al., 1988; Gaffney & Jones, 1989; LeBlanc & Morden, 1991; Li et al., 1991; Doktycz et al., 1992; Paner et al., 1992). However, there has not yet been a complete analysis of sequence effects on thermodynamic stabilities of DNA helixes containing B–Z junctions. Such studies are presented here. The primary goal of this investigation is to examine the effect of B–Z junction formation on the thermal stability of DNA. The oligonucleotides whose sequences are shown in Figure 1 were used in our study. The design of these was based on NMR studies that indicated that the junction region spans base pairs meC:G-7, G:meC-8, and A:T-9 (Sheardy & Winkle, 1989) for BZ–I. For the oligomers discussed in this report, the A:T base pair at position 9 and the G:C base at position 12 are conserved while the base pairs at positions 10 and 11 are varied via permutations of C and T. Although these permutations alter both the sequence and base composition of the oligomers, the A-pyr-pyr-G motif for positions 9–12 in the upper strand is maintained in the series of oligonucleotides studied. The effects of these sequence permutations on the thermally induced duplex to single-strand transitions under ionic conditions that favor either the B form or junction-containing form of the oligomers are reported here.

MATERIALS AND METHODS

DNA Oligomers. All component strands of the DNA oligomers shown in Figure 1 were individually synthesized on an Applied Biosystems (Foster City, CA) 380B DNA synthesizer via the phosphoramidite chemistry (Caruthers, 1988) and purified by C18 reverse-phase HPLC as previously described (Sheardy, 1988). Purity of each strand was verified via analytical reverse-phase HPLC and PAGE. Individual duplexes were generated by mixing equal amounts of the complementary strands and heating at 80 °C for 2 min followed by slow cooling. The extinction coefficients, ϵ (L mol^{-1} cm^{-1} in base pairs), were determined (Fasman, 1975) to be BZ–I, 12 950; BZ–II, 12 940; BZ–V, 13 100; BZ–VI, 12 800.

CD Spectropolarimetry. The CD spectra of each oligomer duplex in phosphate buffer (10 mM phosphate, 0.1 mM EDTA, pH 7.0) at a variety of NaCl concentrations were recorded at 25 °C with either an AVIV 20DS or a JASCO J-500A CD spectropolarimeter.

UV/Vis Spectroscopy. The UV/vis spectra of each oligomer duplex in the same phosphate buffer at a variety of NaCl concentrations at 20 °C and 95 °C were recorded with a Gilford Response II UV/vis spectrophotometer equipped with a thermoset cuvette holder.

Optical Melting Studies. The thermally induced denaturation of each DNA oligomer was investigated using two different protocols. For the first set of experiments, the influence of NaCl on the thermal stabilities of these oligomers was considered by determining the T_m of each oligomer in 10 mM phosphate buffer at a constant DNA concentration as a function of NaCl concentration. For these experiments, [DNA] = 4.4×10^{-5} M (in base pairs) and the NaCl concentration ranged from 15 mM to 5.0 M. The second set of experiments determined the influence of DNA concentration on thermal stability at 115 mM NaCl and 4.5 M NaCl for all oligomers. These salt concentrations were chosen because all oligomers are essentially B-form DNA at 115 mM NaCl and are completely transformed to the B–Z junction form at 4.5 M NaCl. Although most denaturation experiments using short oligonucleotides are carried out at 1.0 M NaCl (Breslauer et al., 1986; Gaffney & Jones, 1989; LeBlanc & Morden, 1991), this concentration of NaCl was not chosen for these studies since there is a slight conformational transition for these oligomers even at 1.0 M NaCl (Sheardy et al., 1993). For these experiments, the DNA concentration ranged from ca. 2×10^{-5} to ca. 1×10^{-3} M.

For each experiment, the denaturation temperature was determined by monitoring the absorbance at 268 nm as the temperature was ramped from 20 °C to 95 °C at ca 0.3 °C/min using the Temperature Programming software of the Gilford Response II. The absorbance of each sample was read every 0.1 °C after 10 consecutive identical temperature readings of the thermoset holder by the spectrometer. A wavelength scan of each sample was also recorded before and after the temperature ramp (i.e. at 20 °C and 95 °C, respectively). After slow cooling back to 20 °C, another wavelength scan was recorded and compared to the original 20 °C scan. If the absorbance of the oligomer at 260 nm in the postrun 20 °C scan differed by more the 2% from that for the prerun scan, that particular experiment was discarded and repeated.

For both sets of experiments focusing on thermal denaturation, the upper and lower baselines were determined graphically from the A_{268} vs T plots, and the T_m was determined from mid-point of the transition (i.e. at $\alpha = 0.5$). For the second set of experiments concerned with the effect of DNA concentration on thermal stability, $1/T_m$ vs ln $C_T/4$ (where C_T is total strand concentration) plots were constructed to determine the van't Hoff enthalpies and entropies, $\Delta H_{vH}°$ and $\Delta S_{vH}°$, respectively, of helix denaturation (Marky & Breslauer, 1987). At least seven data points were collected over the DNA concentration range for these plots. For non-self-complementary duplexes, the relationship between T_m and DNA concentration (C_T) is given by

$$1/T_m = (R/\Delta H_{vH}°) \ln C_T/4 + \Delta S_{vH}°/\Delta H_{vH}° \quad (1)$$

Linear least-squares fits of the data plotted according to eq 1 provide a slope of $R/\Delta H_{vH}°$ and a y-intercept of $\Delta S_{vH}°/\Delta H_{vH}°$, from which $\Delta H°$ and $\Delta S°$ may be calculated. Calculation of the standard Gibb's free energy of helix

denaturation follows from the standard relation:

$$\Delta G_{vH}^\circ = \Delta H_{vH}^\circ - T\Delta S_{vH}^\circ \quad (2)$$

Calculation of ΔG°_{cal}. The van't Hoff analysis described above allows evaluation of the experimentally determined thermal melting free energies (i.e. ΔG°_{exp}). The dinucleotide permutations in the sequence of the oligomers in Figure 1 alter both the hydrogen-bonding scheme and base stacking in the region adjacent to the junction. These alterations will influence the magnitudes of the thermal melting free energies. Doktycz et al. (1992) recently published a method to *predict* thermal melting free energies (i.e. ΔG°_{cal}), for direct comparisons to the experimentally derived values, and takes into account stacking and hydrogen-bonding contributions. By using this method, the contribution of base stacking free energies for these oligomers may be calculated

$$\Delta G_{stack}(j,g) = \sum_i N_i(j)\delta G_i(g) \quad (3)$$

where ΔG_{stack} is the total stacking free energy of oligomer j in solvent g, $N_i(j)$ is the number of times an n-n bp doublet appears in the sequence of oligomer j, and $\delta G_i(g)$ is the deviation from average stacking, in solvent g, associated with that doublet. The δG_i values used were obtained from Table 3 of Doktycz et al. (1992).

The contribution of hydrogen bonding to the total calculated ΔG° can be evaluated using

$$\Delta G_{hb}(j,g) = \Delta S[N_{AT}(j)(T_{AT}(g) - T) + N_{GC}(j)(T_{GC}(g) - T)] \quad (4)$$

where $\Delta G_{hb}(j,g)$ is the total free energy of hydrogen bonding in oligomer j in solvent g, ΔS is the change in entropy of hydrogen-bond formation (which is independent of sequence and sodium ion concentration and is equal to –24.8 cal/kmol (Delcourt & Blake, 1991)), $N_{AT}(j)$ and $N_{GC}(j)$ are the numbers of AT and GC base pairs in sequence j, $T_{AT}(g)$ and $T_{GC}(g)$ are the melting temperatures of AT and GC base pairs in solvent g, and T is the reference temperature. For these calculations, the solvent is 115 mM in NaCl and the reference temperature is 310 K. In order to calculate T_{AT} and T_{GC}, the following equations are used:

$$T_{AT} = 355.55 + 7.95 \ln[Na^+] \quad (5)$$

$$T_{GC} = 391.55 + 4.89 \ln[Na^+] \quad (6)$$

For these calculations, we only considered the stacking and hydrogen bonding for the four base pairs involved in the permutations at positions 9–12 since the contributions to stacking and hydrogen bonding from the other base pairs will be identical from oligomer to oligomer. This is quite reasonable since we are ultimately concerned with the *differences* in free energies within the series.

To illustrate the method, the calculation for the central base paired region of BZ–I (-**ACTG**-) is demonstrated:

$$\Delta G_{stack} = \delta G_{AC} + \delta G_{CT} + \delta G_{TG} \quad (7)$$

Using the published δG_{n-n} values at [NaCl] = 115 mM for AC, CT, and TG stacks (Doktycz et al., 1992), ΔG_{stack} is evaluated to be +33.8 cal/mol. The hydrogen bonding contribution at 115 mM NaCl and T = 310 K is evaluated using eqs 4–6 to be –4915.4 cal/mol. Hence, $\Delta G^\circ_{cal} = \Delta G_{stack} + \Delta G_{hb}$ = –4881.6 cal/mol and represents the melting free energy of base pairs 9–12 in BZ–I.

RESULTS

CD Studies. The CD spectra of BZ–II in low salt (115 mM NaCl) and high salt (4.5 M NaCl) are shown in Figure

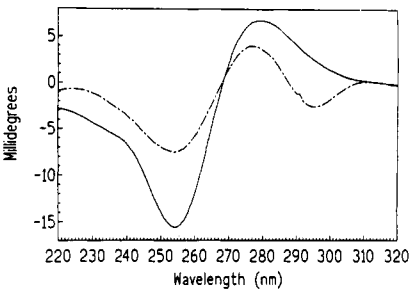

FIGURE 2: The CD spectra at 25 °C of BZ–II ([DNA] 5.4 × 10^{-5} M in base pairs) in 10 mM phosphate buffer at pH 7.0 and 115 mM NaCl (solid line) or 4.5 M NaCl (dashed line). The low-salt spectrum indicates that the oligomer assumes a fully right-handed conformation (B form) while the high-salt spectrum indicates that the oligomer possesses both a left-handed and right-handed conformation (BZ hybrid form) and hence a B–Z junction.

2. The low-salt spectrum is characterized by a deep trough at 255 nm and a peak at 280 nm while the high-salt spectrum is characterized by a shallow trough at 255 nm, a peak at 278 nm, and a very shallow trough at 295 nm. These spectra, as well as those for BZ–V and BZ–VI, are nearly identical to those of BZ–I which has been shown to possess a B–Z conformational junction at high salt (Sheardy, 1988; Sheardy & Winkle, 1989; Doktycz et al., 1990; Sheardy et al., 1993). Under low-salt conditions, each oligomer is a right-handed double helix (i.e. B form). As the concentration of NaCl increases, the oligomer undergoes a conformational transition such that it contains both a right-handed segment and a left-handed segment (i.e. BZ hybrid form) at high salt and, hence, a B–Z junction.

Optical Melting Studies. Figure 3 shows a representative set of melting profiles for BZ–V at constant DNA concentration and NaCl concentrations ranging from 25 to 815 mM (panel A) and from 1.94 to 4.50 M (panel B). Panel 3C shows the melting profiles for BZ–V in 115 mM NaCl at the DNA concentration noted in the figure legend. The denaturation appears in all cases to be a simple two-state process. Plots of T_m vs [NaCl] for all four oligomers (at constant DNA concentration), over the entire range of NaCl concentrations, are shown in Figure 4. Table 1 lists selected T_m values for these oligomers. In all cases, the T_m rises to a maximum at about 1.0 M NaCl, but then decreases the NaCl concentration is further increased.

Plots of T_m vs log [NaCl], over the entire range of NaCl concentrations, for all oligomers are shown in Figure 5. Least squares linear regression analyses of the low-salt data resulted in high correlation factors ($r > 0.9965$) over the range 15–215 mM NaCl for all oligomers. The slopes obtained for the low-salt data are shown in Table 1. Inclusion of additional data from 405 to 815 mM NaCl resulted in successively poorer fits. Likewise, linear regression analyses of the high-salt data resulted in high correlation factors ($r > 0.9975$) over the range 2.56–5.00 M NaCl with successively poorer fits if the 1.60–1.95 M data is included. The slopes of the lines for the low-salt data are nearly identical (average value of 16.9–0.3) for all oligomers studied as are the slopes of the lines for the high-salt data (average value of -27.5 ± 0.2). The results of the linear least-squares analysis of these plots are available as supplementary material. These results suggest that the NaCl is influencing the oligomers in similar fashions in the low-salt range (i.e. below 215 mM NaCl) and in the high-salt range (i.e. above 2.56 M NaCl). An indication of the [NaCl] needed to obtain the maximum T_m can be extrapolated from the intersection of the two lines. The average values for this

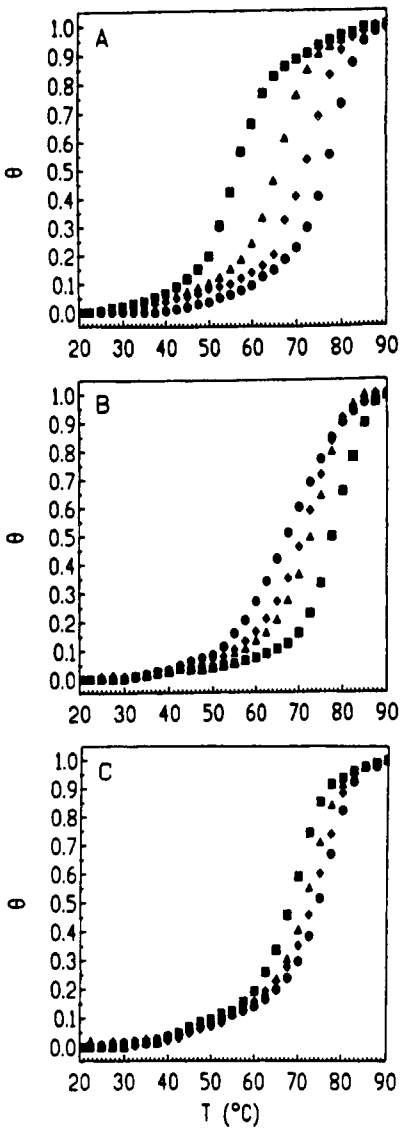

FIGURE 3: Typical set of melting profiles for BZ–V. Plotted is θ vs T where $\theta = [A - A_i]/[A_f - A_i]$ and A is the absorbance at temperature T, A_i is the absorbance at the initial temperature (20 °C), and A_f is the absorbance at the final temperature (95 °C). All thermal denaturations were monitored at λ = 268 nm. (A) BZ–V ([DNA] = 4.4×10^{-5} M in base pairs) in 10 mM phosphate, pH 7.0 buffer with [NaCl] of 25 mM (■), 65 mM (▲), 215 mM (◆), and 800 mM (●); (B) BZ–V ([DNA] = 4.4×10^{-5} M in base pairs) in phosphate buffer with [NaCl] = 1.94 M (■), 2.55 M (▲), 3.78 M (◆), and 4.50 M (●); and (C) BZ–V in phosphate buffer with [NaCl] = 115 mM and [DNA] of 3.6×10^{-5} M (■), 2.0×10^{-4} M (▲), 4.5×10^{-4} M (◆), and 9.1×10^{-4} M (●) in base pairs.

intersection occurs at 1.04 ± 0.02 M NaCl for these oligomers.

Plots constructed according to eq 1 for all oligomers under both low salt (115 mM NaCl) and high salt (4.5 M NaCl) are shown in Figure 6. The slopes and y-intercepts (available as supplementary material) of the least-squares linear regression lines calculated for these plots were used to determine the thermodynamic parameters listed in Table 2. As can be seen, differences in the experimentally determined $\Delta G°$ values at 37 °C between the various oligomers at both salt concentrations arise from changes in both $\Delta H_{vH}°$ and $\Delta S_{vH}°$. Furthermore, the high-salt forms are destabilized relative to the low-salt form by an average value of nearly 1.2 kcal/mol (i.e. $\Delta\Delta G°$ as shown in Table 2). This destabilization is due to decreases in both $\Delta H°$ and $\Delta S°$. The data in Table 2 indicates that the relative stability order for these molecules, over the entire NaCl concentration range, is BZ–VI > BZ–II > BZ–I > BZ–V.

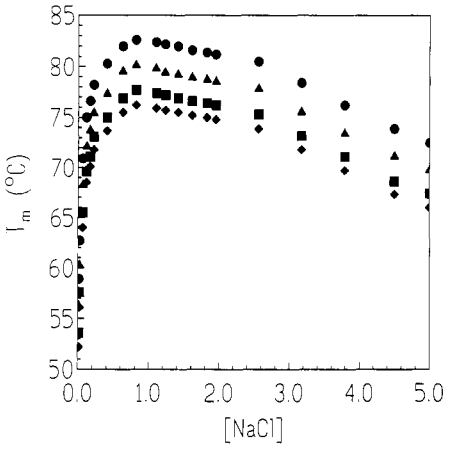

FIGURE 4: The variation of T_m as a function of [NaCl] at [DNA] = 4.4×10^{-5} M in base pairs in 10 mM phosphate, pH 7.0 buffer for BZ–I (■), BZ–II (▲), BZ–V (◆), and BZ–VI (●).

Table 1: The Influence of [NaCl] on the T_m of Junction-Forming Molecules

oligomer	T_m (°C) at [NaCl] indicated[a] 15 mM	115 mM	815 mM	4.50 M	$\delta T_m/\delta$ log [NaCl][b]
BZ-I	53.6	69.6	77.7	68.6	16.9 ± 0.3
BZ-IUNME	56.1	69.4	NA	68.7	14.2 ± 0.3
BZ-II	56.3	72.2	80.2	71.2	16.7 ± 0.3
BZ-V	52.2	68.5	76.2	67.3	17.2 ± 0.3
BZ-VI	58.9	75.0	82.6	73.9	16.9 ± 0.3

[a] Experimental T_m values reported are ±0.3 °C. [b] Obtained over the range of 15–215 mM NaCl.

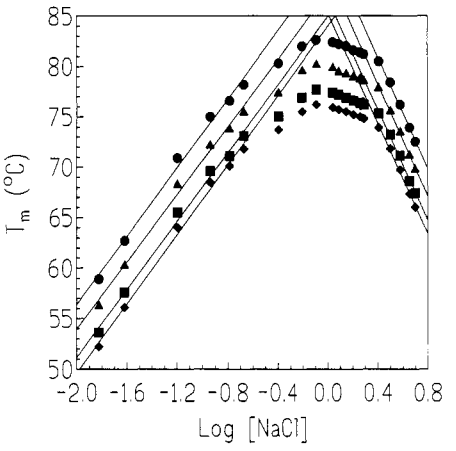

FIGURE 5: The variation of T_m of BZ–I (■), BZ–II (▲), BZ–V (◆), and BZ–VI (●) (all at [DNA] = 4.4×10^{-5} M in base pairs) in 10 mM phosphate, pH 7.0 buffer as a function of log [NaCl] over the entire NaCl concentration range. Least-squares linear regression analysis of the data from 15 to 215 mM NaCl and from 2.56 to 4.5 M NaCl resulted in high correlation fits (resultant lines are drawn). The full set of line parameters are available as supplementary material.

A comparison of the experimentally determined $\Delta G°$ values to values calculated according to the algorithm developed by Doktycz et al. (1992) was carried out. The results of the calculations are given in Table 3. We calculate that the **-ATTG-** stack in BZ–V is the most stable, followed by the **-ATCG-** of BZ–II, the **-ACTG-** stack of BZ–I, and finally the **-ACCG-** stack in BZ–VI. Calculation of the hydrogen-bonding free energies indicates the following order BZ–VI > BZ–II = BZ–I > BZ–V for total hydrogen bond stability. Thus, even though BZ–V is more stably stacked than BZ–VI, hydrogen bonding is the predominant factor in the favored overall stability of BZ–VI. Furthermore, since the hydrogen bonding is similar for BZ–I and BZ–II, the difference in the experimentally determined $\Delta G°$ between these two is entirely

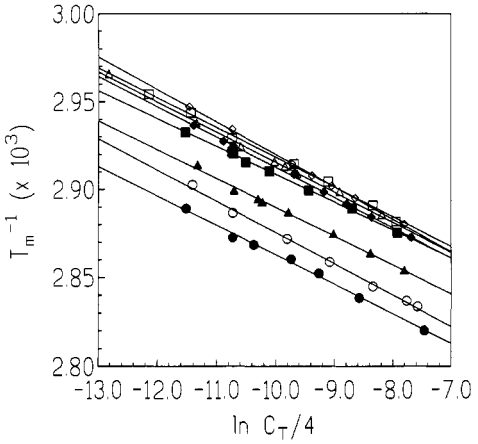

FIGURE 6: The van't Hoff plots ($1/T_m$ vs ln $C_T/4$) for BZ–I (■), BZ–II (▲), BZ–V (■), and BZ–VI (●) in 115 mM NaCl, 10 mM phosphate, pH 7.0 buffer; and BZ–I (□), BZ–II (△), BZ–V (◇), and BZ–VI (○) in 4.5 M NaCl, 10 mM phosphate, pH 7.0 buffer. Line parameters for these plots are available as supplementary material.

Table 2: Thermodynamic Parameters for Junction-Forming Molecules[a]

oligomer	$\Delta H°$ (kcal/mol)	$\Delta S°$ (eu)	$\Delta G°$ (kcal/mol)[b]
	A. In 115 mM NaCl		
BZ-I	126 ± 2	347 ± 7	18.4 ± 0.3
BZ-IUNME	134 ± 1	370 ± 4	19.3 ± 0.2
BZ-II	121 ± 2	330 ± 5	18.7 ± 0.3
BZ-V	116 ± 1	318 ± 4	17.4 ± 0.2
BZ-VI	119 ± 2	321 ± 6	19.5 ± 0.3
	B. In 4.50 M NaCl		
BZ-I	118 ± 3	325 ± 7	17.3 ± 0.3
BZ-IUNME	125 ± 3	343 ± 7	18.7 ± 0.3
BZ-II	116 ± 2	318 ± 5	17.4 ± 0.2
BZ-V	107 ± 1	293 ± 4	16.2 ± 0.2
BZ-VI	112 ± 1	302 ± 4	18.4 ± 0.2

oligomer	$\Delta\Delta H°$ (kcal/mol)[c]	$\Delta\Delta S°$ (eu)[c]	$\Delta\Delta G°$ (kcal/mol)[c]
BZ-I	8	22	1.1
BZ-IUNME	9	26	0.6
BZ-II	5	12	1.3
BZ-V	9	25	1.2
BZ-VI	7	19	1.1

[a] 1 kcal = 0.239 kJ. [b] $\Delta G°$ values are calculated at 37 °C. [c] The $\Delta\Delta G°$ values are the differences between the low-salt data and the high-salt data.

due to differences in stacking. Using the ΔG_{stack} and ΔG_{hb} values from Table 3, one can calculate $\Delta G°_{cal}$ for each oligomer. The most appropriate way to compare oligomers is to calculate the difference in free energies ($\Delta\Delta G°$) within a series, thereby negating end effects (Doktycz et al., 1992). Table 3 shows a comparison of the calculated $\Delta\Delta G°_{cal}$ values thus obtained with the experimental $\Delta\Delta G°_{exp}$. As can be seen, there is excellent agreement between the two sets of values at 115 mM NaCl. A direct comparison to free energy values calculated by the method of Breslauer et al. (1986) was not possible since their particular values were determined at 1.0 M NaCl, a salt concentration at which complete thermodynamic studies were not carried out.

The studies described above were carried out to assess the influence of those base permutations on the thermodynamic stabilities of the oligomers under the two different NaCl concentrations. The salt conditions chosen were such that the conformations of the oligomers would either be fully B form (115 mM NaCl) or in the hybrid BZ form (4.5 M NaCl). In order to assess the influence of the hybrid BZ structures on the thermodynamic stabilities, we carried out a similar set

Table 3: Comparisons of Experimental and Calculated Thermodynamic Values[a] for Duplex Stabilities

oligomer	$\Delta G°_{stack}$ (cal/mol)	$\Delta G°_{hb}$ (cal/mol)	$\Delta G°_{cal}$ (cal/mol)	$\Delta\Delta G°_{cal}$ (kcal/mol)	$\Delta\Delta G°_{exp}$ (kcal/mol)
BZ-I	+33.8	−4915.4	−4881.6	0.0	0.0
BZ-II	−194.6	−4915.4	−5110.0	+0.2	+0.3
BZ-V	−268.6	−3858.9	−4127.5	−0.8	−1.0
BZ-VI	+86.6	−5971.8	−5885.2	+1.0	+1.1

[a] $\Delta G°_{stack}$ and $\Delta G°_{hb}$ are the *calculated* free energies of stacking and hydrogen bonding, respectively, for base pairs 8–11 for these oligomers at 115 mM NaCl as described in Materials and Methods. $\Delta G°_{cal}$, the total calculated free energy of *formation* of those base pairs, is simply the sum of the stacking and hydrogen bonding contributions. $\Delta\Delta G°_{cal}$ values are calculated by subtracting the $\Delta G°_{cal}$ of the oligomer under consideration from $\Delta G°_{cal}$ of BZ-I. These values will be equivalent to the differences in *total* free energies of duplex formation between the oligomers since the contributions from the other base pairs to their total free energies will be identical. Experimental values ($\Delta\Delta G°_{exp}$) are calculated in a similar manner using the experimentally determined $\Delta G°$ values from Table 2 at 115 mM NaCl. The signs of the values in Table 2 were changed before the calculations since the comparison is for relative duplex stabilities. A negative sign for the $\Delta\Delta G°$ values indicates that the oligomer is less stable than BZ-I.

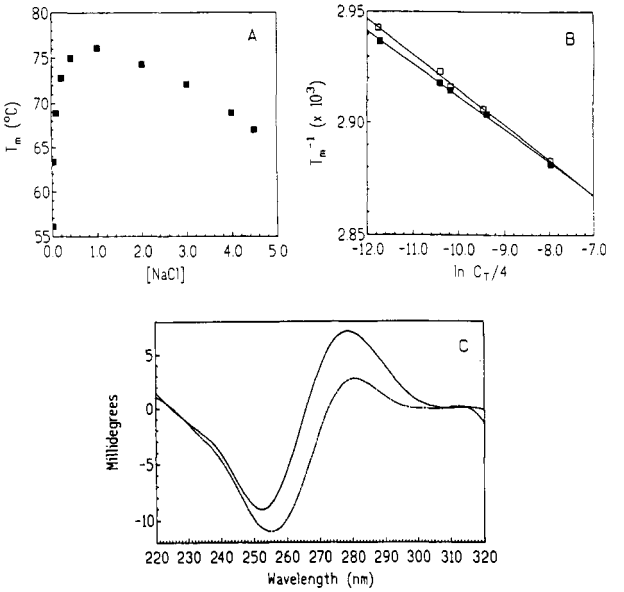

FIGURE 7: (A) The variation of T_m as a function of [NaCl] for BZ–IUNME in 10 mM phosphate, pH 7.0 buffer. (B) The van't Hoff plots ($1/T_m$ vs ln $C_T/4$) for BZ–IUNME in 10 mM phosphate, pH 7.0 buffer at 115 mM NaCl (■) and 4.5 M NaCl (□). Line parameters for these plots are available as supplementary material. (C) The CD spectra at 25 °C of BZ–IUNME ([DNA] = 4.4×10^{-5} M in base pairs) in 10 mM phosphate, pH 7.0 buffer in 115 mM NaCl (solid line) and 4.5 M NaCl (dashed line). The low-salt spectrum indicates a fully right-handed conformation for this oligomer while the high-salt spectrum is typical of a partially dehydrated right-handed conformation (Hanlon et al., 1976; Goto, 1984).

of thermal denaturation studies on BZ–IUNME, an analogue of BZ–I in which the C residues in the Z-forming segment are unmethylated. Demethylation should prevent the B to Z transition of that Z-forming segment (Behe & Felsenfeld, 1981). The general effect of NaCl concentration on the T_m of BZ–IUNME at constant DNA concentration is quite similar to that observed for BZ–I (Figure 7A). Plots constructed according to eq 1 at 115 mM and 4.5 M NaCl also resulted in high correlation linear fits for BZ–IUNME (Figure 7B).

The CD spectra of this oligomer confirms that it is fully right-handed at 115 mM NaCl and does not convert to the hybrid form at 4.5 M NaCl (Figure 7C). The spectrum of BZ–IUNME at 4.5 M NaCl is similar to spectra of DNA polymers and oligomers under high-salt conditions which favor a partially dehydrated right-handed conformation (Hanlon

Table 4: Free Energy of Melting of BZ-I and BZ-IUNME in 0.115 and 4.5 M NaCl[a]

	$\Delta G°$, kcal/mol		
oligomer	0.115 M	4.5 M	$\Delta\Delta G°$
BZ-I	18.4	17.3	−1.1
BZ-IUNME	19.3	18.7	−0.6
$\delta\Delta G°$	0.9	1.4	

[a] All values refer to 25 °C. $\Delta\Delta G°$ is the calculated difference between the 4.5 and 0.115 M NaCl data. $\delta\Delta G°$ is the difference between BZ-IUNME and BZ-I at the same NaCl concentration.

et al., 1976; Goto, 1984; Sheardy et al., 1993). BZ1–UNME does not undergo the salt-induced B to Z transition and hence does not possess a B–Z junction at 4.5 M NaCl. It is thus a suitable control for investigating the effect of the transition to the hybrid BZ form on the stability of BZ–I in high salt.

Analysis of the data presented in Figure 7B resulted in thermodynamic parameters (Table 2) which indicate the BZ–IUNME is more stable than its methylated analogue by 0.9 kcal/mol at low salt and 1.4 kcal/mol at high salt. The difference in stability in BZ–IUNME between the low-salt form and the high-salt form (i.e. $\Delta\Delta G°$ in Table 2) is 0.6 kcal/mol compared to 1.1 kcal/mol for BZ–I. Transition of BZ–I to the hybrid form containing the B–Z junction destabilizes the oligomer by only 0.5 kcal/mol relative to the sequence analogue that does not possess a junction.

DISCUSSION

The primary goal of these studies was to assess the effect of B–Z junction formation on the thermal stability of DNA oligonucleotides. Our results, surprisingly, show (Table 4) that the B–Z junction does *not* destabilize the DNA helix to a significant extent. The presence of the B–Z junction decreases the positive free energy of oligonucleotide melting by at most 1 kcal/mol. An additional striking result to emerge from these studies is a thermodynamic description of the profound effect of slight sequence changes on DNA helix stability. The thermodynamic profiles shown in Table 2 show that alteration of a single dinucleotide step within a 16 bp sequence can significantly alter the energetics of duplex melting. These changes in free energy of helix melting with sequence arises from alteration of both the enthalpy and entropy. These data provide an independent quantitative test of the algorithm presented by Doktycz et al. (1992) for the prediction of DNA helix stability. The agreement between the predicted $\Delta\Delta G°_{cal}$ values and the experimentally determined $\Delta\Delta G°_{exp}$ values is excellent (Table 3).

For all oligonucleotides studied, T_m is a complicated function of NaCl concentration. T_m increases to a maximum value near 1.0 M NaCl and then decreases. Such behavior has been described for native DNA samples (Schildkraut & Lifson, 1965; Gruenwedel et al., 1971; Gruenwedel, 1975). The nonlinear dependence of T_m on NaCl has been proposed to arise from the combined effects of dehydration and anion binding at high salt concentrations (Gruenwedel et al., 1971; Record et al., 1990). More recently, Soumpasis et al. (1990) have used the potentials of mean force (PMF) approach to predict the nonlinear dependence of T_m over a wide range of salt concentration. The behavior predicted by that approach is in basic agreement with the shape of the experimental plots shown in Figure 5, although the magnitudes of the δT_m values are different between the theoretical and experimental values. The situation is even more complicated for the sequences studies here, since in addition to the general polyelectrolyte effects on melting, increasing NaCl alters the conformations of the duplexes. These conformational transitions have been thoroughly studied and described (Sheardy et al., 1993). The 16 bp sequences shown in Figure 1 undergo a transition from a right-handed form in low salt to a hybrid form containing both left- and right-handed regions, and a B–Z junction, at high salt. The transition proceeds through an intermediate I, which probably is a partially dehydrated right-handed form. A phase diagram for these various species has been presented (Sheardy et al., 1993). Of most importance for understanding the NaCl dependence of melting described here, the phase diagram shows that a right-handed conformation is maintained until a Na activity of 2.5 is exceeded. This is well above the maximum at 1.0 M NaCl observed for T_m in Figure 4, so the decrease in T_m cannot be attributed to junction formation alone. Hanlon and co-workers (1976), however, have shown that DNA is dehydrated to a substantial extent in 1.0 M NaCl, lending credence to the proposal (Gruenwedel et al., 1971; Record et al., 1990) that changes in hydration contribute significantly to the decrease in T_m seen in high salt.

Over the range of 15–215 mM NaCl, the increase in T_m may be interpreted in terms of the polyelectrolyte theories of Manning (1978) and Record and co-workers (1978, 1981). We find, from Figure 5, an average value of $(\delta T_m/\delta \log [NaCl]) = 16.9 \pm 0.3$ deg for the oligomers possessing m^5dC. This value reflects the linkage between Na binding and the duplex to single strand transition. Record et al. (1978) have shown that

$$\delta T_m/\delta \log [M] = \{2.303RT_m^2/\Delta H_m\}\Delta n \qquad (8)$$

where T_m is the temperature at the mid-point of the melting transition, [M] is the molar concentration of monovalent counterion, ΔH_m is the enthalpy of the melting transition, R is the gas constant, and Δn is the differential ion binding term. Using the experimental value $(\delta T_m/\delta \log [NaCl]) = 16.9$, along with the enthalpy values and T_m values shown in Tables 1 and 2, an average value of $\Delta n = 3.7$ may be calculated. This value means that 3.7 Na ions are released per 16 bp duplex upon the melting of the helix. This value corresponds to 0.12 Na ions released per phosphate, a value near that observed for the melting of polymeric DNA (Record et al., 1978). Recent studies (Olmsted et al., 1991; 1989) predict deviations from polyelectrolyte theory developed for polymers when using oligonucleotides arising from nonnegligible end effects. The value of $(\delta T_m/\delta \log [NaCl])$ observed here is similar to that reported for polymeric native DNA (Gruenwedel et al., 1971; Gruenwedel, 1975). This similarity in polyelectrolyte behavior of oligonucleotides and polymers, in contrast to the expected deviations, is consistent with the behavior reported by Braunlin and Bloomfield (1991) for the melting of an octanucleotide.

Comparison of the melting experiments performed using BZ–I and its unmethylated counterpart, BZ–IUNME, allows assessment of the effects of both the hybrid conformation possessing the B–Z junction and methylation on DNA thermal stability. These oligonucleotides are identical except for the presence of m^5dC in BZ–I. Table 4 summarizes the pertinent free energy values for the melting of these oligonucleotides in 0.115 and 4.5 M NaCl. In the lower salt, the melting free energy is smaller in magnitude for BZ–I compared to BZ–IUNME, and $\delta\Delta G_{melt}$ is computed to be 0.9 kcal/mol. *Methylation thus destabilizes the double helix.* In the higher salt, $\delta\Delta G_{melt}$ increases in magnitude to 1.4 kcal/mol. This means that the thermal stability of BZ–I, in comparison to BZ–IUNME, is even *lower* in high salt than in low salt. In high salt, BZ–I adopts a hybrid conformation that contains a region of right-handed DNA, the B–Z junction, and a region of left-handed DNA. The decreased thermal stability of the hybrid form relative to the right-handed control sequence BZ–

IUNME in 4.5 M NaCl probably results from the interplay of several factors. For example, the B–Z junction might greatly destabilize the helix, but this might be counterbalanced by a greater thermal stability of the base pairs in the Z conformation. The value of $\delta\Delta G_{melt}$ = 1.4 kcal/mol (Table 4) reflects both the differences in methylation and structures of BZ–I and BZ–IUNME. If we assume the difference in methylation between these two oligonucleotides contributes 0.9 kcal/mol (as observed in 115 mM NaCl) to ΔG_{melt}, then the *overall* effect of the structural difference on the free energy of melting amounts to only 0.5 kcal/mol. That the hybrid form of BZ–I, containing both B- and Z-DNA and the unusual B–Z junction structure, is destabilized by such a small amount is somewhat surprising. The magnitude of the observed destabilization in this case is small in comparison to the destabilizing effect of a bulge on helix stability, which *decreases* the melting free energy by 3–4 kcal/mol (Turner, 1992; LeBlanc & Morden, 1991).

SUMMARY

The principal findings to emerge from our melting studies on five different 16 bp oligonucleotides over a wide range of NaCl concentrations are as follows: (i) Alteration of a single dinucleotide step within a 16 bp sequence profoundly affects the energetics of duplex melting. (ii) Methylation destabilizes the DNA duplex and lowers the free energy of its melting. (iii) The transition to the hybrid BZ structure has a surprisingly small effect on duplex thermal stability and lowers the free energy of melting by only approximately 0.5 kcal/mol relative to the unmethylated control. The effect on the energetics of melting of the transition to the hybrid structure possessing the B–Z junction is thus less than the effect observed resulting from certain dinucleotide sequence changes.

ACKNOWLEDGMENT

The authors wish to thank Neville Kallenbach and Luis Marky for the helpful discussions regarding this work and for the use of their CD spectropolarimeter.

SUPPLEMENTARY MATERIAL AVAILABLE

Tables of the line parameters (i.e. slopes and y-intercepts) for the plots in Figure 5 (T_m vs log [NaCl]) and Figures 6 and 7B ($1/T_m$ vs ln $C_T/4$) (1 page). Ordering information is given on any current masthead page.

REFERENCES

Behe, M., & Felsenfeld, G. (1981) *Proc. Natl. Acad. Sci. U.S.A. 78*, 1619–1623.
Braulin, W. H., & Bloomfield, V. A. (1991) *Biochemistry 30*, 754–758.
Breslauer, K. J., Frank, R., Blocker, H., & Marky, L. A. (1986) *Proc. Natl. Acad. Sci. U.S.A. 83*, 3746–3750.
Caruthers, M. H. (1988) in *Chemical and Enzymatic Synthesis of Gene Fragments* (Gassen, H. G., & Lang, A., Eds.) Verlag Chemie, Weinheim.
Delcourt, S. G., & Blake, R. D. (1991) *J. Biol. Chem. 266*, 15160–15169.
Doktycz, M. J., Benight, A. S., & Sheardy, R. D. (1990) *J. Mol. Biol. 212*, 3–6.
Doktycz, M. J., Goldstein, R. F., Paner, T. M., Gallo, F. J., & Benight, A. S. (1992) *Biopolymers 32*, 849–864.
Fasman, G., Ed. (1975) in *CRC Handbook of Biochemistry and Molecular Biology*, 3rd ed., p 589, CRC Press, Cleveland, OH.
Gaffney, B. L., & Jones, R. A. (1989) *Biochemistry 28*, 5881–5889.
Goto, S. (1984) *Biopolymers 23*, 2211–2222.
Gruenwedel, D. W. (1975) *Biochim. Biophys. Acta 395*, 246–257.
Gruenwedel, D. W., Hsu, G. H., & Lu, D. S. (1971) *Biopolymers 10*, 47–68.
Guo, Q., Lu, M., Sharestanifar, M., Sheardy, R. D., & Kallenbach, N. R. (1991) *Biochemistry 30*, 11735–11741.
Hanlon, S., Brudno, S., Wu, T. T., & Wolf, B. (1976) *Biochemistry 14*, 1648–1660.
Ichikawa, A., Kuboya, T., Aoyama, T., & Sugiura, Y. (1992) *Biochemistry 31*, 6784–6787.
Jacobs, K. A., Rudersdorf, R., Neill, S. D., Dougherty, J. P., Brown, E. L., & Fritsch, E. F. (1988) *Nucleic Acids Res. 16*, 4637–4650.
LeBlanc, D. A., & Morden, K. M. (1991) *Biochemistry 30*, 4042–4047.
Li, Y., Zon, G., & Wilson, W. D. (1991) *Biochemistry 30*, 7566–7572.
Lu, M., Guo, Q., Kallenbach, N. R., & Sheardy, R. D. (1992) *Biochemistry 31*, 4712–4719.
Manning, G. S. (1978) *Q. Rev. Biophys. 11*, 179–246.
Manzini, G., Xodo, L. E., Quadrifoglio, F., van Boom, J. H., & van der Marel, G. A. (1987) *J. Biomol. Struct. Dyn. 4*, 651–662.
Marky, L. A., & Breslauer, K. J. (1987) *Biopolymers 26*, 1601–1620.
Marky, L. A., Blumenfeld, K. S., & Breslauer, K. J. (1988) *Can. J. Chem. 66*, 836–838.
Olmsted, M. C., Anderson, C. F., & Record, M. T., Jr. (1989) *Proc. Natl. Acad. Sci. U.S.A. 86*, 7766–7770.
Olmsted, M. C., Anderson, C. F., & Record, M. T., Jr. (1991) *Biopolymers 31*, 1593–1604.
Paner, T. M., Amaratunga, M., & Benight, A. S. (1992) *Biopolymers 32*, 881–892.
Record, M. T., Jr., Anderson, C. F., & Lohman, T. M. (1978) *Q. Rev. Biophys. 11*, 102–178.
Record, M. T. Jr., Mazur, S. J., Melancon, P., Roe, J. H., Shaner, S. L., & Unger, L. (1981) *Annu. Rev. Biochem. 30*, 997–1021.
Record, M. T., Jr., Olmsted, M., & Anderson, C. F. (1990) in *Theoretical Biochemistry & Molecular Biophysics* (Beveridge, D. L., & Lavery, R., Eds.) pp 285–307, Adenine Press, Guilderland, NY.
Shildkraut, C., & Lifson, S. (1965) *Biopolymers 3*, 195–208.
Senoir, M., Jones, R. A., & Breslauer, K. J. (1988) *Biochemistry 27*, 3879–3885.
Sheardy, R. D. (1988) *Nucleic Acids Res. 16*, 1153–1167.
Sheardy, R. D. (1991) *Spectroscopy 6*, 14–16.
Sheardy, R. D., & Winkle, S. A. (1989) *Biochemistry 28*, 720–725.
Sheardy, R. D., Suh, D., Kurzinsky, R., Doktycz, M. J., Benight, A. S., & Chaires, J. B. (1993) *J. Mol. Biol. 231*, 475–488.
Suh, D., Sheardy, R. D., & Chaires, J. B. (1991) *Biochemistry 30*, 8722–8726.
Soumpasis, D. M., Garcia, A., Klement, R., & Jovin, T. (1990) in *Theoretical Biochemistry & Molecular Biophysics* (Beveridge, D. L., & Lavery, R., Eds.) pp 343–360, Adenine Press, Guilderland, NY.
Turner, D. H. (1992) *Curr. Opinion Struc. Biol. 2*, 334–337.
Winkle, S. A., & Sheardy, R. D. (1990) *Biochemistry 29*, 6514–6521.
Winkle, S. A., Aloyo, M. C., Morales, N., Zambrano, T. Y., & Sheardy, R. D. (1991) *Biochemistry 30*, 10601–10606.